Theory of biphoton generation in a single-resonant optical parametric oscillator far below threshold

Ulrike Herzog, Matthias Scholz, and Oliver Benson
Nano-Optics, Institut für Physik, Humboldt-Universität zu Berlin, D-10117 Berlin, Germany
(Received 19 September 2007; published 28 February 2008)

We present a quantum-theoretical treatment of biphoton generation in single-resonant type-II parametric down-conversion. The nonlinear medium is continuously pumped and is placed inside a cavity which is resonant for the signal field, but nonresonant for the idler deflected by an intracavity polarizing beam splitter. The intensity of the classical pump is assumed to be sufficiently low in order to yield a biphoton production rate that is small compared to the cavity loss rate. Explicit expressions are derived for the rate of biphoton generation and for the biphoton wave function. The output spectra of the signal and idler field are determined, as well as the second-order signal-idler cross-correlation function which is shown to be asymmetric with respect to the time delay. Due to frequency entanglement in the signal-idler photon pair, the idler spectrum is found to reveal the longitudinal mode structure of the cavity, even though the idler field is not resonant.

DOI: 10.1103/PhysRevA.77.023826 PACS number(s): 42.65.Lm, 42.50.Ar, 03.67.−a

I. INTRODUCTION

In parametric down-conversion, a pump photon of frequency ω_p incident on a medium with a second-order nonlinear susceptibility χ is split into two photons with lower frequency [1]. Spontaneous parametric down conversion produces photon pairs that can be entangled in many degrees of freedom [2]. The resulting two-photon state, consisting of a signal photon at frequency ω_s and an idler photon at frequency $\omega_i=\omega_p-\omega_s$, is often called a biphoton. Upon postselection on the idler photons, the process provides a source of heralded single photons which represent the principal resource in many quantum information processing protocols like quantum cryptography [3–5] or linear optics quantum computation [6]. Quantum networks have been proposed [7,8] that rely on stationary atoms or ions as information processing nodes and on single photons to transmit information via optical fibers. First building blocks of this scheme have already been realized [9,10]. For an efficient atom-photon coupling, the photon bandwidth has to match the linewidth of the atomic transition which is by orders of magnitude smaller than the bandwidth of the photons emitted in spontaneous parametric down-conversion.

In order to reduce the photon bandwidth, cavity-enhanced parametric down-conversion can be applied. A bright source of heralded narrow-band single photons was experimentally realized [11] using a double-resonant optical parametric oscillator (OPO). The nonlinear crystal was placed inside a cavity resonant for both the signal and the idler field, and in the output a single narrow-band longitudinal signal mode was selected with an external frequency filter. Clearly, to conditionally achieve single-photon generation, the OPO has to be operated in the regime far below threshold where the production rate of down-converted photons is small compared to the loss rate of the cavity. A number of preceding experiments for biphoton generation in a double-resonant OPO far below threshold have been performed [12–17], and the first theoretical description was given in Ref. [13]. Recently, the theory of the double-resonant OPO has been extended by analyzing the conditionally prepared single-photon state [18] and by providing a multimode treatment which is valid for both pulsed and stationary pump fields [19].

To ensure reliable operation of a quantum network, continuous photon emission over a long period of time is essential. For this purpose, an active stabilization of the OPO is necessary which proves to be a complicated task in the double-resonant case while it is easier to achieve for a single-resonant cavity. Continuous biphoton generation in a single-resonant OPO far below threshold has recently been demonstrated in our group [20] using a setup where only the signal mode experiences resonance enhancement in the cavity while the orthogonally polarized idler mode is nonresonant due to deflection by an intracavity polarizing beam splitter. Additional passive filtering with the help of an external cavity can select a single longitudinal mode and will thus enable the generation of narrow-band single photons.

To our knowledge, a theoretical treatment of the single-resonant OPO far below threshold has not been performed so far. The present paper aims to fill this gap. Based on the concepts of the pioneering theoretical studies of spontaneous parametric down-conversion [21,22], we provide the theoretical background for our experimental results [20]. Different from the approaches used for the theoretical description of the double-resonant OPO [13,18,19], free-field quantization of the idler field is inevitable for our scheme.

This paper is organized as follows. In Sec. II, the basic equations for describing the nonlinear interaction between the quantized signal and idler fields are provided. The biphoton production rate and the biphoton wave functions are derived in Sec. III by applying the standard perturbative treatment in the Schrödinger picture [1]. The results are used in Sec. IV to derive the spectral properties of the emitted radiation and to study the second-order signal-idler cross-correlation function. Section V concludes the paper by establishing the connection to real experimental situations.

II. BASIC EQUATIONS

A. Interaction Hamiltonian

We consider type-II parametric down-conversion in a nonlinear crystal of length l that is pumped by a monochro-

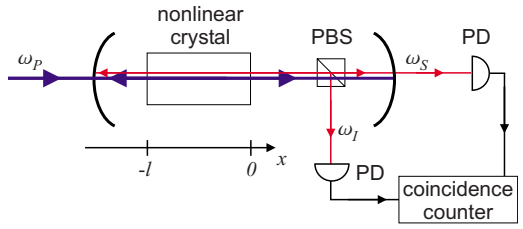

FIG. 1. (Color online) Scheme of the considered experiment. The cavity acts as a one-sided resonator for the signal field, while the idler field is nonresonant due to deflection at an intracavity polarizing beam splitter. The signal-idler cross-correlation function is determined by delayed coincidence detection.

matic linearly polarized classical field of frequency ω_P. The crystal is assumed to be placed inside a cavity which is resonant for the signal field, but not for the idler field, polarized orthogonal to the signal. Figure 1 shows a schematic picture of the corresponding experimental setup [20]. The central frequencies ω_S and ω_I of the signal and idler field depend on the properties of the birefringent nonlinear crystal and are determined by energy and momentum conservation known as phase-matching [1]:

$$\omega_P = \omega_S + \omega_I, \tag{2.1}$$

$$\vec{k}_p(\omega_P) = \vec{k}_s(\omega_S) + \vec{k}_i(\omega_I). \tag{2.2}$$

Here, $\vec{k}_p$, $\vec{k}_s$, and $\vec{k}_i$ are the wave vectors of the pump, signal, and idler waves which are collinear in the considered setup, with the signal leaving the cavity in a positive x direction. The standing-wave fields of the pump and the signal inside the cavity are composed of two components, propagating in a negative and positive x direction, respectively. Because of the phase-matching conditions, only those components contribute to the parametric interaction that have the same propagation direction as the idler wave. Neglecting the vector notation of the fields, the positive-frequency part of the electric field in the relevant component of the classical pump inside the crystal can be written as

$$E_{P,cr}(x,t) = E_P e^{i[k_p(\omega_P)x - \omega_P t]}. \tag{2.3}$$

The weak signal and idler fields inside the crystal are described by the operators $E^{(+)}_{S,cr} = E^{(-)\dagger}_{S,cr}$ and $E^{(+)}_{I,cr} = E^{(-)\dagger}_{I,cr}$, respectively, denoting the positive-frequency part of their copropagating field components. The interaction Hamiltonian can be written in the simplified form

$$H_{int} = \frac{\chi}{2l}\int_{-l}^{0} dx (E_{P,cr}E^{(-)}_{S,cr}E^{(-)}_{I,cr} + E^{*}_{P,cr}E^{(+)}_{S,cr}E^{(+)}_{I,cr}), \tag{2.4}$$

where the second-order nonlinear susceptibility χ is frequency-dependent [1]. Before utilizing Eq. (2.4), we need to find explicit expressions for the operators $E^{(+)}_{S,cr}$ and $E^{(+)}_{I,cr}$.

B. Free-field operators

For later use, we start by providing the operators for the signal and idler fields in free space. The positive-frequency electric field operator of a wave with transverse cross-section A propagating freely in the x direction is given by $E^{(+)}(x,t) = \lim_{L\to\infty} \Sigma_{j=0}^{\infty} \sqrt{\frac{\hbar\omega_j}{2\epsilon_0 LA}} a_j e^{i\omega_j(x/c-t)}$ with $\omega_j = 2\pi jc/L$, where L is the quantization length and a_j denotes the photon annihilation operator of mode j. Let us consider the signal field and introduce the frequency difference $\Omega_j = \omega_j - \omega_S$. Using $\Delta\Omega = 2\pi c/L$, the transition to the continuum limit is performed via the replacement $\Sigma_j a_j \cdots \to (\Delta\Omega)^{-1/2}\int_{-\omega_S}^{\infty} d\Omega a(\omega_S+\Omega)\cdots$, where the continuous field operators $a(\omega)$ have the dimension $s^{1/2}$. Since the bandwidth of the signal is small compared to its central frequency ω_S, the integration interval can be extended to $-\infty$, and we arrive at the approximate operator representation

$$E^{(+)}_S(x,t) = \sqrt{\frac{\hbar\omega_S}{2\epsilon_0 cA}}\int_{-\infty}^{\infty}\frac{d\Omega}{\sqrt{2\pi}} a(\omega_S+\Omega)e^{i(\omega_S+\Omega)(x/c-t)}, \tag{2.5}$$

where [23]

$$[a(\omega_1), a^{\dagger}(\omega_2)] = \delta(\omega_1 - \omega_2). \tag{2.6}$$

Similarly, the corresponding operator for the idler field in free space is given by

$$E^{(+)}_I(x,t) = \sqrt{\frac{\hbar\omega_I}{2\epsilon_0 cA}}\int_{-\infty}^{\infty}\frac{d\Omega}{\sqrt{2\pi}} b(\omega_I+\Omega)e^{i(\omega_I+\Omega)(x/c-t)}, \tag{2.7}$$

where

$$[b(\omega_1), b^{\dagger}(\omega_2)] = \delta(\omega_1 - \omega_2). \tag{2.8}$$

Since in type-II parametric down-conversion signal and idler photons are polarized orthogonally, we have

$$[a(\omega_1), b^{\dagger}(\omega_2)] = 0. \tag{2.9}$$

C. Field operators inside the crystal

We now turn to the fields inside the crystal. If the nonlinear interaction is small, we do not need to consider the complicated problem of field quantization in a nonlinear medium, but we can represent the field operators inside the crystal by adapting the corresponding expressions for the free-field operators in order to account for the presence of a lossless dispersive medium [1]. In accordance with Ref. [24], the operator for the positive-frequency part of the idler field inside the crystal then takes the approximate form

$$E^{(+)}_{I,cr}(x,t) = \sqrt{\frac{\hbar\omega_I}{2\epsilon_0 cAn_I}}\int_{-\infty}^{\infty}\frac{d\Omega}{\sqrt{2\pi}} b(\omega_I+\Omega)e^{i[k_I(\Omega)x - (\omega_I+\Omega)t]}, \tag{2.10}$$

where we introduced the wave vector at frequency $\omega_I+\Omega$,

$$k_I(\Omega) = \frac{\omega_I+\Omega}{c} n_i(\omega_I+\Omega). \tag{2.11}$$

Here, the replacements $\epsilon_0 \to \epsilon_0 n_i^2$ and $c \to c/n_i$ have been performed where n_i is the refractive index of the idler wave and $n_I = n_i(\omega_I)$.

To describe the signal field, we have to take the presence of the resonator into account. Let us first assume a lossless resonator completely filled with the nonlinear medium. The quantization length of the field is then equal to the crystal length l. When n_s denotes the refractive index of the signal, the adapted resonator eigenfrequencies characterizing the longitudinal modes can be written as

$$\omega_m = \frac{(m_0+m)\pi c}{n_s(\omega_m)l} \quad \text{with} \quad m_0 = \frac{\omega_S n_S l}{\pi c}, \tag{2.12}$$

where $n_S = n_s(\omega_S)$, $m = 0, \pm 1, \pm 2, \ldots$ and $m_0 \gg |m|$. Since the frequency difference between adjacent modes is small compared to the total spectral width of the signal, as will become obvious in Sec. IV, we can assume without lack of generality that ω_S coincides with the frequency of a longitudinal mode and m_0 is an integer, i.e., that the cavity is tuned to resonance. Using the Taylor expansion $n_s(\omega_m) = n_S + (\omega_m - \omega_S)\frac{\partial n_s}{\partial \omega}|_{\omega=\omega_S}$, we find from Eq. (2.12) after minor algebra that

$$\omega_m \approx \omega_S + m\frac{\pi v_{g,S}}{l} \equiv \omega_S + m\Delta\omega_c, \tag{2.13}$$

where

$$v_{g,S} = \frac{c}{n_S + \omega_S \left.\dfrac{\partial n_s}{\partial \omega}\right|_{\omega=\omega_S}} \tag{2.14}$$

is the group velocity of the signal at frequency ω_S. By adapting the empty-cavity field operator [23] with the replacements $\epsilon_0 \to \epsilon_0 n_s^2$ and $c \to c/n_s$, the part of the standing-wave signal field operator inside the crystal that corresponds to a component traveling in a positive x direction in the lossless resonator is found to be

$$E_{S,cr}^{(+)}(x,t) = \sqrt{\frac{\hbar\omega_S \Delta\omega_c}{\epsilon_0 n_S c A \pi}} \sum_{m=-\infty}^{\infty} a_m \frac{e^{i\omega_m[x/cn_s(\omega_m)-t]}}{2}. \tag{2.15}$$

Here, we replaced the quantization length under the square-root sign by the expression $l = \pi v_{g,S}/\Delta\omega_c \approx \pi c/(n_S \Delta\omega_c)$, following Eqs. (2.13) and (2.14). Moreover, the summation has been extended to $m = -\infty$, in analogy to the expanded integration range in Eq. (2.5). The photon annihilation and creation operators for mode m obey the usual commutation relation $[a_m, a_{m'}^\dagger] = \delta_{m,m'}$.

When resonator losses are incorporated, the modes turn into quasimodes and the annihilation operators a_m in Eq. (2.15) become time-dependent. According to the input-output formalism [23,25] for a one-sided cavity with loss constant γ, the damping of mode m is described by

$$\dot{a}_m(t) = -\frac{\gamma}{2} a_m(t) + \sqrt{\gamma} a_m^{IN}(t). \tag{2.16}$$

The operators $a_m^{IN}(t)$ and $a_m^{OUT}(t)$ characterize the ingoing and outgoing photon flux at frequency ω_m and have the dimension $s^{-1/2}$. They are related by the boundary condition

$$a_m^{IN}(t) = \sqrt{\gamma} a_m(t) - a_m^{OUT}(t). \tag{2.17}$$

In order to determine $a_m(t)$, we use the representation

$$a_m^{OUT}(t) = \frac{1}{\sqrt{2\pi}} \int_{-\infty}^{\infty} d\Omega a(\omega_m + \Omega) e^{-i\Omega t}, \tag{2.18}$$

where, in analogy to Eq. (2.6),

$$[a(\omega_m + \Omega), a^\dagger(\omega_{m'} + \Omega')] = \delta_{m,m'} \delta(\Omega - \Omega'). \tag{2.19}$$

Equation (2.19) implies that the quasimodes do not overlap which is justified in the good-cavity limit

$$\gamma \ll \Delta\omega_c. \tag{2.20}$$

After inserting Eq. (2.17) into Eq. (2.16), we obtain by Fourier transformation the solution

$$a_m(t) = \frac{1}{\sqrt{2\pi}} \int_{-\infty}^{\infty} d\Omega a(\omega_m + \Omega) \frac{\sqrt{\gamma}}{\frac{\gamma}{2} + i\Omega} e^{-i\Omega t}, \tag{2.21}$$

which has to be applied to Eq. (2.15). The operator for the relevant field component of the signal in the lossy cavity can then be written as

$$E_{S,cr}^{(+)}(x,t) = \sqrt{\frac{\hbar\omega_S}{2\epsilon_0 n_S c A}} \frac{\sqrt{\gamma\Delta\omega_c}}{2\pi} \sum_{m=-\infty}^{\infty} \int_{-\infty}^{\infty} d\Omega \frac{a(\omega_m+\Omega)}{\frac{\gamma}{2} + i\Omega} \times e^{i[k_{S,m}(\Omega)x - (\omega_m+\Omega)t]}. \tag{2.22}$$

Here,

$$k_{S,m}(\Omega) = \frac{\omega_m + \Omega}{c} n_s(\omega_m + \Omega) \tag{2.23}$$

is the wave vector corresponding to a traveling-wave component of frequency $\omega_m + \Omega$. The denominator in the integral in Eq. (2.22) describes radiation suppression for frequencies ω with $|\omega - \omega_m| = |\Omega| \gg \gamma$ while resonance enhancement occurs for $\omega \approx \omega_m$.

So far, we have assumed a resonator length L_r that coincides with the crystal length l. If $L_r > l$, a rigorous quantization of the signal field has to account for the exact position of the crystal inside the resonator, but is beyond the scope of the present paper. For the purposes of our approximative treatment, however, it is sufficient to describe the signal field inside the crystal by Eq. (2.22) with $\Delta\omega_c = \Delta\omega$ and $\omega_m = \omega_S + m\Delta\omega$, where $\Delta\omega$ is the effective free spectral range. The latter can be represented as

$$\Delta\omega = \frac{2\pi}{T} \quad \text{with} \quad T = \frac{2l}{v_{g,S}} + \frac{2(L_r - l)}{c}, \tag{2.24}$$

where T is the effective cavity round-trip time of a signal photon.

III. RATE OF BIPHOTON GENERATION AND THE BIPHOTON WAVE FUNCTION

With the expressions for the operators of the signal and idler field at hand, we are now in the position to specify the

interaction Hamiltonian and to derive a perturbative solution of the Schrödinger equation. Making use of Eqs. (2.1), (2.3), (2.10), and (2.22), as well as Eq. (2.13) with $\Delta\omega_c \to \Delta\omega$, and taking the frequency-dependence of the nonlinear susceptibility into account, we find from Eq. (2.4)

$$H_{int} = i\hbar\alpha \sum_{m=-\infty}^{\infty} \int_{-\infty}^{\infty} d\Omega \frac{\sqrt{\gamma}}{\frac{\gamma}{2} - i\Omega} \int_{-\infty}^{\infty} d\Omega' F_m(\Omega,\Omega') \times a^\dagger(\omega_m + \Omega) b^\dagger(\omega_I + \Omega') e^{i(m\Delta\omega+\Omega+\Omega')t} + \text{H.a.}, \tag{3.1}$$

where we introduced the function

$$F_m(\Omega,\Omega') = \frac{\chi(\omega_P;\omega_m+\Omega,\omega_I+\Omega')}{\chi(\omega_P;\omega_S,\omega_I)l} \int_{-l}^{0} dx e^{i[k_P - k_{S,m}(\Omega) - k_I(\Omega')]} \tag{3.2}$$

and defined the constant

$$\alpha = \frac{-iE_P}{8\pi\epsilon_0 cA} \sqrt{\frac{\omega_S\omega_I}{n_S n_I}} \chi(\omega_P;\omega_S,\omega_I)\sqrt{\Delta\omega}. \tag{3.3}$$

We are interested in the regime far below threshold where the biphoton production rate κ is much smaller than the cavity damping rate,

$$\kappa \ll \gamma, \tag{3.4}$$

and the mean photon number in the resonator is therefore close to zero. Since the mean time interval between biphoton emission events is large compared to the cavity damping time, the resonator can be assumed to be empty before each emission event. For this case, we can perform a perturbative treatment of the nonlinear interaction, assuming that at the initial time $t=0$, the combined signal-idler field is in the vacuum state, described by $|0\rangle = |0\rangle_S \otimes |0\rangle_I$. In the following we rely on the ideas developed for the theory of spontaneous parametric down-conversion [1,21,22]. By expanding the formal solution of the time-dependent Schrödinger equation, up to a normalization factor, the state vector describing the combined signal-idler field at a time $t=\Delta t \ll \kappa^{-1}$ is found to be $|\psi(\Delta t)\rangle \propto |0\rangle + |\tilde{\psi}(\Delta t)\rangle$ with

$$|\tilde{\psi}(\Delta t)\rangle = \frac{1}{i\hbar} \int_0^{\Delta t} dt H_{\text{int}}(t)|0\rangle. \tag{3.5}$$

After substituting Eq. (3.1) into Eq. (3.5), integration with respect to t yields

$$|\tilde{\psi}(\Delta t)\rangle = \sum_{m=-\infty}^{\infty} \int_{-\infty}^{\infty} d\Omega \frac{\alpha\sqrt{\gamma}}{\frac{\gamma}{2} - i\Omega} \int_{-\infty}^{\infty} d\Omega' F_m(\Omega,\Omega')\Delta t \times \text{sinc}\left[\frac{1}{2}(m\Delta\omega + \Omega + \Omega')\Delta t\right] \times e^{i/2(m\Delta\omega+\Omega+\Omega')\Delta t} a^\dagger(\omega_m+\Omega) b^\dagger(\omega_I+\Omega')|0\rangle, \tag{3.6}$$

where we used the sinc-function defined as $\text{sinc}(z) = \frac{\sin z}{z}$ with $\text{sinc}(0) = 1$.

The nonnormalized vector $|\tilde{\psi}(\Delta t)\rangle$ refers to the state of the radiation field on the condition that a signal-idler photon pair has been produced during the time interval Δt. Since this condition applies with the probability $\langle\tilde{\psi}(\Delta t)|\tilde{\psi}(\Delta t)\rangle$, the biphoton production rate is given by

$$\kappa = \frac{1}{\Delta t}\langle\tilde{\psi}(\Delta t)|\tilde{\psi}(\Delta t)\rangle. \tag{3.7}$$

Applying the commutation relations, Eqs. (2.8) and (2.19), we get from Eq. (3.6)

$$\langle\tilde{\psi}(\Delta t)|\tilde{\psi}(\Delta t)\rangle = (\Delta t)^2 \sum_{m=-\infty}^{\infty} \int_{-\infty}^{\infty} d\Omega \frac{|\alpha|^2\gamma}{\left(\frac{\gamma}{2}\right)^2 + \Omega^2} \times \int_{-\infty}^{\infty} d\Omega' |F_m(\Omega,\Omega')|^2 \times \text{sinc}^2\left[\frac{1}{2}(m\Delta\omega + \Omega + \Omega')\Delta t\right]. \tag{3.8}$$

Because of the properties of the sinc function, the integral is dominated by the region $m\Delta\omega + \Omega + \Omega' \leq \pi/\Delta t$. If Δt is sufficiently large and $F_m(\Omega,\Omega')$ is a slowly varying function of Ω' in this region, the latter function can be replaced by its value at $\Omega' = -m\Delta\omega - \Omega$ [1]. Using the relation $\int_{-\infty}^{\infty} \text{sinc}^2(z) dz = \pi$, the integration with respect to Ω' is then readily performed, and we obtain

$$\langle\tilde{\psi}(\Delta t)|\tilde{\psi}(\Delta t)\rangle = 2\pi|\alpha|^2\Delta t \sum_{m=-\infty}^{\infty} \int_{-\infty}^{\infty} d\Omega \frac{\gamma}{\left(\frac{\gamma}{2}\right)^2 + \Omega^2} |\Phi_m(\Omega)|^2, \tag{3.9}$$

where

$$\Phi_m(\Omega) = F_m(\Omega, -m\Delta\omega - \Omega). \tag{3.10}$$

For further evaluation, we need to specify the function $\Phi_m(\Omega)$. Using Eqs. (2.2), (2.11), and (2.23) with $\omega_m = \omega_S + m\Delta\omega$, Taylor expansion around the central frequencies ω_S and ω_I yields

$$k_P - k_{S,m}(\Omega) - k_I(-m\Delta\omega - \Omega) \approx (m\Delta\omega + \Omega)\frac{\tau_0}{l}, \tag{3.11}$$

where we introduced the time constant

$$\tau_0 = \frac{l}{c}\left(n_I + \omega_I \frac{\partial n_i}{\partial\omega}\bigg|_{\omega=\omega_I} - n_S - \omega_S \frac{\partial n_s}{\partial\omega}\bigg|_{\omega=\omega_S}\right). \tag{3.12}$$

The latter is equivalent to

$$\tau_0 = \frac{l}{v_{g,I}} - \frac{l}{v_{g,S}} \tag{3.13}$$

and describes the difference between the transit times of a signal and idler photon through a crystal of length l, originating from the difference in the signal and idler group velocities, $v_{g,S}$ and $v_{g,I}$, defined by Eq. (2.14) and by the corresponding equation for the idler wave, respectively. Since in any real experiment $|v_{g,S}-v_{g,I}| \ll v_{g,S}$, it follows that $|\tau_0| \ll (\Delta\omega)^{-1}$ where we used Eq. (2.24). Hence we are considering a parameter range in this problem that is characterized by the combined inequality

$$\kappa \ll \gamma \ll \Delta\omega \ll |\tau_0|^{-1}, \tag{3.14}$$

where Eqs. (2.20) and (3.4) have been incorporated [27]. Assuming a constant nonlinear susceptibility within the bandwidth given by $|\tau_0|^{-1}$, we find from Eqs. (3.10), (3.11), and (3.2) that

$$\Phi_m(\Omega) \approx \frac{1}{l}\int_{-l}^{0} dx e^{i(m\Delta\omega+\Omega)\tau_0/lx}. \tag{3.15}$$

In order to determine the rate of biphoton generation, we have to insert Eq. (3.15) into Eq. (3.9) where the integration with respect to Ω is effectively restricted to the cavity bandwidth γ with $\gamma \ll \Delta\omega$. Hence we neglect Ω compared to $m\Delta\omega$ in Eq. (3.15) for $m \neq 0$. Moreover, Eq. (3.14) implies $|\Omega\tau_0| \ll 1$ in the relevant interval $|\Omega| \lesssim \gamma$ and therefore $\Phi_0(\Omega) \approx 1$. After integration with respect to x, we get the approximation

$$\Phi_m(\Omega) \approx \Phi_m(0) = \mathrm{sinc}\left(m\Delta\omega\frac{\tau_0}{2}\right)e^{-im\Delta\omega\tau_0/2}, \tag{3.16}$$

which can be used in connection with Eqs. (3.9), (3.7), and (3.3) to determine the rate of biphoton generation,

$$\kappa = \left(\frac{\chi|E_p|}{4\epsilon_0 cA}\right)^2 \frac{\omega_S\omega_I}{n_S n_I}\Delta\omega \sum_{m=-\infty}^{\infty} \mathrm{sinc}^2\left(m\Delta\omega\frac{\tau_0}{2}\right). \tag{3.17}$$

Further simplification is possible if we transform the sum into an integral with respect to $z = m\Delta\omega\tau_0/2$, introducing the positive increment $dz = \Delta\omega|\tau_0|/2$ where $dz \ll 1$ because of Eq. (3.14). We then arrive at the expression

$$\kappa \approx \left(\frac{\chi|E_p|}{4\epsilon_0 cA}\right)^2 \frac{\omega_S\omega_I}{n_S n_I}\frac{2\pi}{|\tau_0|} \tag{3.18}$$

that does not depend on the properties of the resonator because the mean photon number in our cavity is approximately zero and, in addition, an associated idler mode exists for each signal mode which meets the requirement for energy conservation.

The presented perturbative treatment relies on the condition $|\tau_0| \ll \Delta t \ll \kappa^{-1}$ so that the wave function $|\tilde{\psi}(\Delta t)\rangle$ in Eq. (3.6) and the approximation leading to Eq. (3.9) are valid simultaneously. The normalized vector $|\psi\rangle = (\kappa\Delta t)^{-1/2}|\tilde{\psi}(\Delta t)\rangle$ can be denoted as the biphoton wave function since it represents the state of the radiation field on the condition that exactly one signal-idler photon pair is present.

A more convenient representation of the biphoton wave function is obtained if the sinc-function in Eq. (3.6) is replaced by $2\pi\delta(m\Delta\omega+\Omega+\Omega')$ according to the standard procedure [22]. Mathematically, this corresponds to the limit $\Delta t \to \infty$, implying $\kappa \to 0$; then the integration with respect to Ω' can be performed immediately. In analogy to the expression given in Ref. [22], we obtain the biphoton wave function

$$|\psi\rangle = \mathcal{N}\sum_{m=-\infty}^{\infty}\int_{-\infty}^{\infty} d\Omega \frac{\Phi_m(\Omega)}{\frac{\gamma}{2}-i\Omega} a^\dagger(\omega_S + m\Delta\omega + \Omega) \times b^\dagger(\omega_I - m\Delta\Omega - \Omega)|0\rangle, \tag{3.19}$$

where $\Phi_m(\Omega)$ is given by Eq. (3.15) and $\mathcal{N}$ is a normalization constant. The explicit value of $\mathcal{N}$ [26] is not important as long as only normalized quantities characterizing the radiation field are considered. Equation (3.19) clearly reveals the frequency-entanglement between the signal and idler photon and will serve as our basic equation to determine the properties of the emitted radiation.

IV. PROPERTIES OF THE EMITTED RADIATION

A. Output spectra of the signal and idler field

First we investigate the output spectra $S_S(\omega)$ and $S_I(\omega)$ of the signal and idler field, defined as

$$S_{S/I}(\omega) = \frac{1}{2\pi}\int_{-\infty}^{\infty} d\tau G^{(1)}_{S/I}(\tau)e^{i\omega\tau}, \tag{4.1}$$

where $G^{(1)}_S(\tau)$ and $G^{(1)}_I(\tau)$ are the first-order temporal correlation functions of the respective fields outside the resonator. In the following, it is convenient to use the Heisenberg picture and to start from the expression

$$G^{(1)}_{S/I}(\tau) = \langle\psi|E^{(-)}_{S/I}(x,t)E^{(+)}_{S/I}(x,t+\tau)|\psi\rangle. \tag{4.2}$$

Here, $|\psi\rangle$ is the time-independent biphoton wave function given by Eq. (3.19) and $E^{(+)}_S = E^{(-)\dagger}_S$ and $E^{(+)}_I = E^{(-)\dagger}_I$ denote the positive-frequency parts of the time-dependent operators of the electric fields in free space, given by Eqs. (2.5) and (2.7). Let us first determine the spectrum of the idler field. Considering

$$b(\omega_I + \Omega')b^\dagger(\omega_I - m\Delta\omega - \Omega)|0\rangle = \delta(\Omega' + m\Delta\omega + \Omega)|0\rangle, \tag{4.3}$$

due to Eq. (2.8), we obtain from Eqs. (2.7) and (3.19)

$$E^{(+)}_I(x,t)|\psi\rangle \propto \sum_{m=-\infty}^{\infty}\int_{-\infty}^{\infty} d\Omega \frac{\Phi_m(\Omega)}{\frac{\gamma}{2}-i\Omega} \times e^{i(\omega_I - m\Delta\omega - \Omega)(x/c-t)}a^\dagger(\omega_S + m\Delta\omega + \Omega)|0\rangle. \tag{4.4}$$

By taking the inner product of $E^{(+)}_I(x,t+\tau)|\psi\rangle$ and $E^{(+)}_I(x,t)|\psi\rangle$ and applying the commutation relation Eq. (2.19), we find

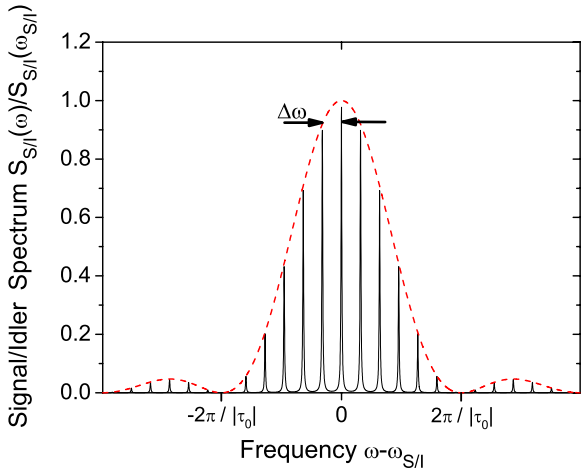

FIG. 2. (Color online) Schematic plot of the normalized signal and idler output spectra. The width of the Lorentzian peaks is determined by the cavity damping rate γ, and they are separated by the free spectral range $\Delta\omega=2\pi/T$. The envelope, described by the sinc-function in Eq. (4.6), yields the total spectral width $2\pi/|\tau_0|$.

$$G_I^{(1)}(\tau) \propto \sum_{m=-\infty}^{\infty} \int_{-\infty}^{\infty} d\Omega \frac{|\Phi_m(\Omega)|^2}{\left(\frac{\gamma}{2}\right)^2 + \Omega^2} e^{-i(\omega_I - m\Delta\omega - \Omega)\tau}. \quad (4.5)$$

In analogy to the derivation of Eq. (3.17), the dependence of Φ_m on Ω can be neglected within the relevant bandwidth determined by γ. After inserting Eq. (3.16) into Eq. (4.5), the Fourier transform yielding the idler spectrum according to Eq. (4.1) is readily performed. The signal spectrum can be determined in a completely analogous way, and we finally arrive at the relation

$$S_{S/I}(\omega) \propto \sum_{m=-\infty}^{\infty} \frac{\mathrm{sinc}^2\left(m\Delta\omega\frac{\tau_0}{2}\right)}{\left(\frac{\gamma}{2}\right)^2 + (\omega_{S/I} - m\Delta\omega - \omega)^2}. \quad (4.6)$$

Equation (4.6) indicates that both the signal and idler spectrum are composed of Lorentzians of half-width γ centered at frequencies $\omega_{S/I}-m\Delta\omega$ with $m=0,\pm1,\ldots$ where the respective spectral envelopes are determined by the sinc-function in the nominator. From Fig. 2 it becomes obvious that the frequency bandwidth of the signal and idler photons is characterized by $|\tau_0|^{-1}$. Their temporal uncertainty is thus equal to the modulus of the time constant τ_0 introduced in Eq. (3.12) and resulting from the phase-matching conditions. Even though the idler wave is not resonant, the longitudinal mode structure of the resonator is revealed in the idler spectrum due to the frequency entanglement between the signal and idler photon which arises from the interaction underlying the biphoton generation process.

B. Signal-idler cross-correlations

The coincidence rate for detecting an idler photon at time t and a signal photon at time $t+\tau$, both at equal distance from the end facet of the crystal, is proportional to the temporal correlation function

$$G_{IS}^{(2)}(\tau) = \langle\psi|E_I^{(-)}(x,t)E_S^{(-)}(x,t+\tau)E_S^{(+)}(x,t+\tau)E_I^{(+)}(x,t)|\psi\rangle, \quad (4.7)$$

where again $E_S^{(+)}$ and $E_I^{(+)}$ are the free-field operators defined by Eqs. (2.5) and (2.7). With the explicit expression for the biphoton wave function $|\psi\rangle$, given by Eq. (3.19), we get

$$E_S^{(+)}(x,t+\tau)E_I^{(+)}(x,t)|\psi\rangle \propto e^{i[(\omega_S+\omega_I)(x/c-t)-\tau\omega_S]} \sum_{m=-\infty}^{\infty} e^{-im\Delta\omega\tau} \int_{-\infty}^{\infty} d\Omega \frac{\Phi_m(\Omega)}{\frac{\gamma}{2} - i\Omega} e^{-i\Omega\tau}|0\rangle, \quad (4.8)$$

where Eq. (4.3) and the corresponding relation for the signal modes

$$a(\omega_S+\Omega')a^\dagger(\omega_S+m\Delta\omega+\Omega)|0\rangle = \delta(\Omega'-m\Delta\omega-\Omega)|0\rangle, \quad (4.9)$$

following from Eq. (2.6), have been applied. According to Eq. (4.7), the correlation function $G_{IS}^{(2)}(\tau)$ is proportional to the squared norm of the Hilbert vector on the right-hand side of Eq. (4.8). It can be determined from the explicit expression for $\Phi_m(\Omega)$, given by Eq. (3.15), together with the integral identities

$$-\frac{1}{\pi}\int_{-\infty}^{\infty} d\Omega \frac{e^{-i\Omega t}}{\frac{\gamma}{2} - i\Omega} = \begin{cases} 0 & \text{if } t<0 \\ 1 & \text{if } t=0 \\ 2e^{-\gamma/2t} & \text{if } t>0. \end{cases} \quad (4.10)$$

First, it is important to observe that

$$G_{IS}^{(2)}(\tau) = 0 \quad \text{if} \quad \tau + \frac{\tau_0}{2} < -\frac{|\tau_0|}{2}, \quad (4.11)$$

which is equivalent to $\tau<-\tau_0$ for $\tau_0>0$ and $\tau<0$ for $\tau_0<0$, respectively. Mathematically, Eq. (4.11) is due to the expression $\Omega t=\Omega(\tau-\frac{x}{l}\tau_0)$ which results from inserting Eq. (3.15) into Eq. (4.8) and is negative in the given case for any x inside the crystal, i.e., for $-l\le x\le 0$. Therefore the upper line of Eq. (4.10) applies. Physically, the correlation function vanishes because the arrival time of the signal photon in a photon pair can precede the arrival time of the corresponding idler photon at most by a time interval that is within the temporal uncertainty interval $|\tau_0|$ inherent in the biphoton generation process.

On the other hand, the presence of the resonator allows a signal photon to be detected considerably later than the associated idler photon since the signal photon may bounce back and forth between the resonator mirrors repeatedly before leaving the resonator. For time delays τ outside the limits of Eq. (4.11), we approximate $\Phi_m(\Omega)$ by Eq. (3.16) where the integration with respect to x has been performed and the dependence on Ω has been neglected. After inserting Eq. (3.16) into Eq. (4.8), the damping of the cavity gives rise to a factor proportional to $e^{-\gamma/2\tau}$ for $G_{IS}(\tau)\neq 0$, which follows

from the third line of Eq. (4.10) [28]. Since $G_{IS}^{(2)}(\tau)=\|E_S^{(+)}\times(x,t+\tau)E_I^{(+)}(x,t)|\psi\rangle\|^2$, we finally get from Eq. (4.8) the approximate result

$$G_{IS}^{(2)}(\tau) \propto e^{-\gamma\tau}\left|\sum_{m=-\infty}^{\infty}\mathrm{sinc}\left(m\Delta\omega\frac{\tau_0}{2}\right)e^{-im\Delta\omega(\tau+\tau_0/2)}\right|^2$$

$$\text{if} \quad \tau+\frac{\tau_0}{2}\geq-\frac{|\tau_0|}{2}. \tag{4.12}$$

According to Eq. (3.13), the sign of τ_0 is determined by the relation between the signal and idler group velocities, i.e., $\tau_0>0$ for $v_{g,S}>v_{g,I}$ and $\tau_0<0$ for $v_{g,S}<v_{g,I}$. A numerical evaluation reveals that Eq. (4.12) describes a decaying periodic function with peaks of width $|\tau_0|$ centered at $\tau=jT-\tau_0/2$, where $j=0,1,\ldots$ and $T=2\pi/\Delta\omega$ is the cavity round-trip time. The time shift $-\tau_0/2$ of the peaks arises since for $\tau_0>0$ the time needed by the center of the signal wave packet to travel from the middle of the crystal to its end facet is by the amount $\tau_0/2$ shorter than the time needed by the center of the idler wave packet to cover the same distance while the opposite holds for $\tau_0<0$.

Transforming the sum in Eq. (4.12) into an integral, the expression for the signal-idler cross-correlation function can be further approximated, in analogy to the procedure applied to derive Eq. (3.18). Introducing $z=m\Delta\omega\tau_0/2$ and $dz=\Delta\omega\tau_0/2$, we find that $G_{IS}^{(2)}(\tau)\propto e^{-\gamma\tau}I^2$ with $I=\int_{-\infty}^{\infty}\mathrm{sinc}(z)\cos(az)dz$ since $\mathrm{sinc}(z)$ is an even function of z. Because of the periodicity of the cosine function, the parameter a can be written as $a=1+2[\tau-([\frac{\tau}{T}]+1)T]/\tau_0$ where $[\frac{\tau}{T}]$ denotes the largest integer that does not exceed τ/T. Since $I=\pi$ for $|a|<1$ and $I=0$ for $|a|>1$, Eq. (4.12) takes a simple form that can be combined with Eq. (4.11) to yield the compact approximate representation

$$G_{IS}^{(2)}(\tau) \propto \sum_{j=0}^{\infty}\begin{cases} e^{-\gamma jT} & \text{if} \quad \left|\tau-jT+\frac{\tau_0}{2}\right|\leq\frac{|\tau_0|}{2} \\ 0 & \text{else,}\end{cases} \tag{4.13}$$

where $j=|[\frac{\tau}{T}]|$ (see Fig. 3). Here, we took into account that due to Eq. (3.14) cavity damping is negligible during the time interval $|\tau_0|$, i.e., $\exp(-\gamma\tau_0)\approx 1$.

V. DISCUSSION AND CONCLUSIONS

In a real experiment, the sharp peaks of the function $G_{IS}^{(2)}(\tau)$ will be broadened due to the finite resolution time of the detector setup. When the latter is taken into account by performing the convolution with respect to a Gaussian function, Eq. (4.13) yields the time-averaged cross-correlation function

$$\overline{G_{IS}}^{(2)}(\tau) \propto \sum_{j=0}^{\infty}\exp\left[-\gamma jT-\frac{4(jT-\tau)^2}{(\Delta T)^2}\right], \tag{5.1}$$

where ΔT characterizes the effective resolution time and where we have assumed $\Delta T\gg|\tau_0|$. The resulting averaged function is plotted in Fig. 4 for two different values of ΔT. A second-order cross-correlation function showing the behavior of the solid line in Fig. 4 has recently been measured in our group [20], and the results have been found to be in excellent agreement with the predictions derived from Eqs. (4.11) and (4.12).

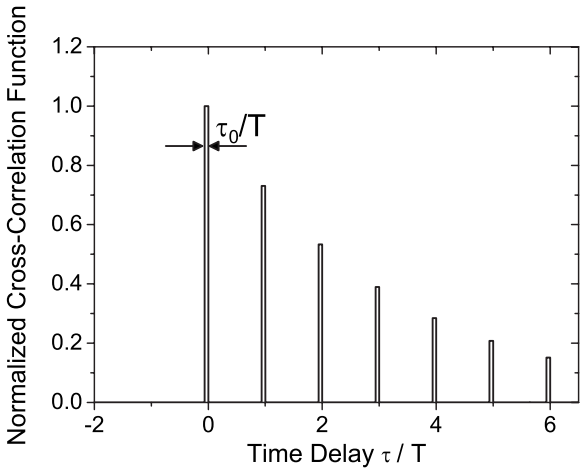

FIG. 3. Schematic representation of the normalized second-order signal-idler cross-correlation function $G_{IS}^{(2)}(\tau)$ according to Eq. (4.13) for $\tau_0>0$ and $\gamma/\Delta\omega=0.05$. If the time delay τ is equal to zero or multiples of the cavity round-trip time $T=2\pi/\Delta\omega$, the function exhibits pronounced peaks which decay with the cavity damping time γ^{-1}.

We still note that for spontaneous parametric down-conversion in a double-resonant cavity the signal-idler cross-correlation function has also been found to exhibit a comb-like structure which is, however, symmetric with respect to the time delay [14–16]. The effect has been explained by applying the concept of mode locking to the frequency-entangled biphoton state, pointing out that due to the large coherence time of the pump, photon pairs with different frequencies have a common phase and form a coherent superposition [14].

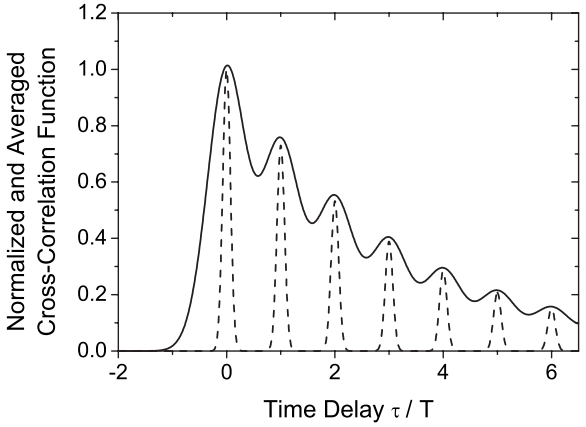

FIG. 4. Time-averaged second-order signal-idler cross-correlation function $\overline{G_{IS}}^{(2)}(\tau)$ for $\gamma/\Delta\omega=0.05$. The ratio between the resolution time ΔT and the cavity round-trip time $T=2\pi/\Delta\omega$ is assumed as $\Delta T/T=0.02$ (dashed line) and $\Delta T/T=1$ (solid line), respectively.

To summarize, we performed a theoretical investigation of biphoton generation by spontaneous parametric down-conversion in a single-resonant OPO far below threshold. We derived analytical expressions for the rate of biphoton generation, for the output spectra of the signal and idler fields, as well as for the second order signal-idler cross-correlation function. Our investigations provide the theoretical background for explaining the results of a recent experiment [20], where stable continuous operation of a single-resonant OPO far below threshold has been demonstrated.

ACKNOWLEDGMENTS

This work was supported by Deutsche Forschungsgemeinschaft DFG, Grant No. BE 2224/5. M. Scholz acknowledges funding by Deutsche Telekom Stiftung.

[1] L. Mandel and E. Wolf, *Optical Coherence and Quantum Optics* (Cambridge University Press, Cambridge, England, 1995).
[2] J. T. Barreiro, N. K. Langford, N. A. Peters, and P. G. Kwiat, Phys. Rev. Lett. **95**, 260501 (2005).
[3] C. M. Bennett and G. Brassard, in *Proceedings of the IEEE Conference on Computers, Systems, and Signal Processing in Bangalore, India* (IEEE, New York, 1984), p. 175.
[4] N. Gisin, Rev. Mod. Phys. **74**, 145 (2002).
[5] E. Waks, K. Inoue, C. Santori, D. Fattal, J. Vučković, G. S. Solomon, and Y. Yamamoto, Nature (London) **420**, 762 (2002).
[6] E. Knill, R. Laflamme, and G. J. Milburn, Nature (London) **409**, 46 (2001).
[7] S. Lloyd, M. S. Shahriar, J. H. Shapiro, and P. R. Hemmer, Phys. Rev. Lett. **87**, 167903 (2001).
[8] J. I. Cirac, P. Zoller, H. J. Kimble, and H. Mabuchi, Phys. Rev. Lett. **78**, 3221 (1997).
[9] C. W. Chou, J. Laurat, H. Deng, K. S. Choi, H. de Riedmatten, D. Felinto, and H. J. Kimble, Science **316**, 1316 (2007).
[10] T. Wilk, S. C. Webster, A. Kuhn, and G. Rempe, Science **317**, 488 (2007).
[11] J. S. Neergaard-Nielsen, B. Melholt Nielsen, H. Takahashi, A. I. Vistnes, and E. S. Polzik, Opt. Express **15**, 7940 (2007).
[12] Z. Y. Ou and Y. J. Lu, Phys. Rev. Lett. **83**, 2556 (1999).
[13] Y. J. Lu and Z. Y. Ou, Phys. Rev. A **62**, 033804 (2000).
[14] Y. J. Lu, R. L. Campbell, and Z. Y. Ou, Phys. Rev. Lett. **91**, 163602 (2003).
[15] H. Wang, T. Horikiri, and T. Kobayashi, Phys. Rev. A **70**, 043804 (2004).
[16] C. E. Kuklewicz, F. N. C. Wong, and J. H. Shapiro, Phys. Rev. Lett. **97**, 223601 (2006).
[17] C. E. Kuklewicz, M. Fiorentino, G. Messin, F. N. C. Wong, and J. H. Shapiro, Phys. Rev. A **69**, 013807 (2004).
[18] A. E. B. Nielsen and K. Mølmer, Phys. Rev. A **75**, 023806 (2007).
[19] A. E. B. Nielsen and K. Mølmer, Phys. Rev. A **76**, 033832 (2007).
[20] M. Scholz, F. Wolfgramm, U. Herzog, and O. Benson, Appl. Phys. Lett. **91**, 191104 (2007).
[21] C. K. Hong and L. Mandel, Phys. Rev. A **31**, 2409 (1985).
[22] R. Ghosh, C. K. Hong, Z. Y. Ou, and L. Mandel, Phys. Rev. A **34**, 3962 (1986).
[23] D. F. Walls and G. J. Milburn, *Quantum Optics* (Springer, Berlin, 1994).
[24] K. J. Blow, R. Loudon, S. J. D. Phoenix, and T. J. Shepherd, Phys. Rev. A **42**, 4102 (1990).
[25] M. J. Collett and C. W. Gardiner, Phys. Rev. A **30**, 1386 (1984).
[26] For completeness, we state the formal result $\mathcal{N}^2 = |\alpha|^2 2\pi\gamma/[\kappa\delta(0)]$ which follows with the help of Eqs. (2.19), (3.7), and (3.9). The delta function arises since $\langle 0|b(\omega)b^\dagger(\omega)|0\rangle = \delta(0)$ because of Eq. (2.8). Note that $\kappa \to 0$.
[27] In a typical experiment [20], the relevant parameters are given by $\kappa \sim 0.1$ MHz, $\gamma \sim 10$ MHz, $\Delta\omega \sim 1$ GHz, and $|\tau_0|^{-1} \sim 150$ GHz.
[28] Since a mathematically exact treatment of the discontinuity is physically irrelevant, we replace the value of the integral in the second line of Eq. (4.10) by the value of the third line.